Magnetic Field Dependence of the Adiabatic Susceptibility Tensor of Powdered Cerium Magnesium Nitrate

B. M. Abraham, J. B. Ketterson, and P. R. Roach

Argonne National Laboratory, Argonne, Illinois 60439

(Received 5 July 1972)

The magnetic field dependence of the components of the adiabatic susceptibility tensor of powdered and single-crystal specimens of cerium magnesium nitrate have been measured in the Curie-law limit. The single-crystal results are in good agreement with thermodynamic calculations, while the powdered results show deviations at higher fields. The smallness of the field dependence of the perpendicular component of the susceptibility tensor suggests its use in thermometry at low temperatures in finite magnetic fields. The coefficient in the asymptotic expression for the heat capacity $C_M = b/T^2$ is found to be $b/R = 6.16 \pm 0.1$ (mK)^2.

I. INTRODUCTION

The thermodynamic treatment of the ac susceptibility of a paramagnetic salt in the presence of a static external magnetic field was given by Casimir and du Pré.[1] In the adiabatic limit (where the spin system cannot relax to be in equilibrium with the lattice) and for a material with an isotropic g factor, they found that the component of the magnetic susceptibility parallel to the external field is given by

$$\chi_{\shortparallel} = \frac{c}{T} \frac{g^2}{4} \left(1 + \frac{cg^2 H^2}{4b} \right)^{-1} ,$$

where c is the Curie constant defined $N\mu_B^2/k_B$, and the spin specific heat is $C_M = b/T^2$. The remaining symbols have their conventional meanings. As given here, this expression is valid in the Curie-law limit. It is also known, under the above restrictions, that the diagonal components of the susceptibility tensor in a plane perpendicular to the field axis are independent of the field[2] [Eq. (9a) of Sec. II].

It would be useful to have an expression for the effect of a magnetic field on a powdered specimen, in particular, powder formed from crystallites of a material with an anisotropic g factor, such as cerium magnesium nitrate (CMN). This salt plays an important role in low-temperature thermometry and must often be powdered in order to make thermal contact with either an experimental apparatus or with liquid ^{3}He and ^{3}He-^{4}He solutions. A knowledge of the effect of an applied field on the susceptibility would permit one to make corrections for the apparent shift in the temperature if measurements were made in the presence of an external field.

In Sec. II, we derive the susceptibility tensor for a powdered salt with an axis of symmetry and a g factor isotropic in the plane perpendicular to that axis—the case with CMN. We shall show that the field dependence of the perpendicular components

of the susceptibility tensor for such a system do not vanish; the perpendicular components are, however, considerably smaller than the parallel component (for CMN they are approximately eight times smaller). In Sec. III, we present a series of experimental measurements, which are then compared with the theory. In the course of these measurements, a more accurate value for the coefficient b in the expression for the specific heat was determined.

II. THEORY

In this section we derive an expression for the adiabatic susceptibility tensor of a powdered specimen of CMN. We proceed as follows. (1) We first calculate the adiabatic susceptibility tensor in a coordinate system that is aligned with the CMN crystal coordinates but with the static field in an arbitrary direction. (2) Next we transform the susceptibility tensor by rigid-body rotations involving the Euler angles into a coordinate system with the new z axis aligned parallel to the magnetic field. (3) Finally we average over the Euler angles to obtain the required results for a powder.

The first law of thermodynamics for a magnetic system is given by

$$dQ = dU - \vec{H} \cdot d\vec{M} , \qquad (1)$$

where Q is the heat transferred, U is the internal energy, $\vec{H}$ is the magnetic field, and $\vec{M}$ is the magnetization. The adiabatic condition requires $dQ = 0$. The change in internal energy is given by $dU = C_M dT$, where C_M is the heat capacity. Equation (1) then becomes

$$dT = (1/C_M) \vec{H} \cdot d\vec{M} . \qquad (2)$$

From the magnetic equation of state $\vec{M} = \vec{M}(\vec{H}, T)$, we can compute

$$d\vec{M} = \left(\frac{\partial \vec{M}}{\partial \vec{H}} \right)_T \cdot d\vec{H} + \left(\frac{\partial \vec{M}}{\partial T} \right)_{\vec{H}} dT . \qquad (3)$$

Eliminating dT between Eqs. (2) and (3), we obtain

$$\overleftrightarrow{\chi}_S \equiv \left(\frac{\partial \vec{M}}{\partial \vec{H}}\right)_S = \left[1 - \frac{1}{C_M}\left(\frac{\partial \vec{M}}{\partial T}\right)_{\vec{H}} \vec{H}\right]^{-1} \cdot \left(\frac{\partial \vec{M}}{\partial \vec{H}}\right)_T . \quad (4)$$

The low-lying energy levels of the spin system in CMN are given by $E_n = \pm\frac{1}{2}\mu_B(g_\perp^2 H_x^2 + g_\perp^2 H_y^2 + g_\parallel^2 H_z^2)^{1/2}$; here μ_B is the Bohr magneton while $g_\parallel$ and $g_\perp$ are the trigonal axis and basal plane g factors, respectively. From the free energy $F = -NkT \ln\sum_n e^{-E_n/kT}$, we can calculate the magnetization $\vec{M} = \partial F/\partial \vec{H}$; in the Curie-law limit, we find

$$M_x = \frac{1}{4}cg_\perp^2 (H_x/T) , \quad (5a)$$

$$M_y = \frac{1}{4}cg_\perp^2 (H_y/T) , \quad (5b)$$

$$M_z = \frac{1}{4}cg_\parallel^2 (H_z/T) . \quad (5c)$$

For the temperature range of interest ($T > 15$ mK) the heat capacity of CMN is given approximately by $C_M = b/T^2$, where b is an experimentally determined constant. From Eqs. (4) and (5) and the heat capacity we can calculate the adiabatic susceptibility tensor in the crystal coordinate system. The result is

$$\overleftrightarrow{\chi}_S = \frac{c/T}{1 + (c/4b)(g_\perp^2 H_x^2 + g_\perp^2 H_y^2 + g_\parallel^2 H_z^2)}$$

$$\times \begin{bmatrix} \frac{1}{4}g_\perp^2[1 + (c/4b)(g_\perp^2 H_y^2 + g_\parallel^2 H_z^2)] & -(cg_\perp^4/16b)H_x H_y & (cg_\perp^2 g_\parallel^2/16b)H_x H_z \\ -(cg_\perp^4/16b)H_x H_y & \frac{1}{4}g_\perp^2[1 + (c/4b)(g_\perp^2 H_x^2 + g_\parallel^2 H_z^2)] & -(cg_\perp^2 g_\parallel^2/16b)H_y H_z \\ -(cg_\perp^2 g_\parallel^2/16b)H_x H_z & -(cg_\perp^2 g_\parallel^2/16b)H_y H_z & \frac{1}{4}g_\parallel^2[1 + (cg_\perp^2/4b)(H_x^2 + H_y^2)] \end{bmatrix} . \quad (6)$$

This completes the first part of our calculation.

The orientation of an individual crystallite in a powdered sample may be specified by the Euler angles φ, θ, and ψ. Equation (6) gives the susceptibility tensor in the crystal coordinate system (x, y, z) and we must determine the corresponding tensor in the laboratory coordinate system (x', y', z'). The z' axis is parallel to the magnetic field axis and is specified by the polar angles φ and θ; thus $H_x = \cos\varphi \sin\theta$, $H_y = \sin\varphi \sin\theta$, $H_z = \cos\theta$. The ψ degree of freedom corresponds to a rotation of the crystallite about the magnetic field axis. A vector $\vec{r}$ in the crystal coordinate system is transformed into a vector $\vec{r}'$ in the laboratory system by the Euler matrix $\overleftrightarrow{R}$; i.e., $\vec{r}' = \overleftrightarrow{R} \cdot \vec{r}$, where $\overleftrightarrow{R}$ is given by[3]

$$\overleftrightarrow{R} = \begin{bmatrix} \cos\varphi \cos\theta \cos\psi - \sin\varphi \sin\psi & \sin\varphi \cos\theta \cos\psi + \cos\varphi \sin\psi & -\sin\theta \cos\psi \\ -\cos\varphi \cos\theta \sin\psi - \sin\varphi \cos\psi & -\sin\varphi \cos\theta \sin\psi + \cos\varphi \cos\psi & \sin\theta \sin\psi \\ \cos\varphi \sin\theta & \sin\varphi \sin\theta & \cos\theta \end{bmatrix} . \quad (7)$$

The susceptibility in the laboratory frame is then given by

$$\overleftrightarrow{\chi}_S' = \overleftrightarrow{R} \cdot \overleftrightarrow{\chi}_S \cdot \overleftrightarrow{\tilde{R}} \quad (8)$$

where $\overleftrightarrow{\tilde{R}}$ is the transpose of $\overleftrightarrow{R}$.

The powdered specimen must have macroscopic rotational symmetry about the magnetic field axis; thus, the averaged susceptibility tensor is diagonal with the basal plane components equal. It is then sufficient to calculate only $(\overleftrightarrow{\chi}_S')_{x'x'}$ and $(\overleftrightarrow{\chi}_S')_{z'z'}$. After some calculation we obtain

$$(\overleftrightarrow{\chi}_S')_{x'x'} = \frac{cg_\perp^2}{4T}\sin^2\psi$$

$$+ \frac{(c/4T)(g_\perp^2\cos^2\theta + g_\parallel^2\sin^2\theta + (cH^2/4b)g_\perp^2 g_\parallel^2)}{1 + (cH^2/4b)(g_\perp^2\sin^2\theta + g_\parallel^2\cos^2\theta)}\cos^2\psi , \quad (9a)$$

$$(\overleftrightarrow{\chi}_S')_{z'z'} = \frac{(c/4T)(g_\perp^2\sin^2\theta + g_\parallel^2\cos^2\theta)}{1 + (cH^2/4b)(g_\perp^2\sin^2\theta + g_\parallel^2\cos^2\theta)} . \quad (9b)$$

We must now average Eqs. (9a) and (9b) over all possible orientations of the crystallites. Thus

$$\chi_\perp \equiv \langle \overleftrightarrow{\chi}_S' \rangle_{x'x'} = (1/8\pi^2)\int_0^{2\pi}\int_0^{2\pi}\int_0^\pi (\overleftrightarrow{\chi}_S')_{x'x'}\sin\theta\, d\theta\, d\varphi\, d\psi , \quad (10a)$$

$$\chi_\parallel \equiv \langle \overleftrightarrow{\chi}_S' \rangle_{z'z'} = (1/4\pi)\int_0^{2\pi}\int_0^\pi (\overleftrightarrow{\chi}_S')_{z'z'}\sin\theta\, d\theta\, d\varphi . \quad (10b)$$

On performing the above integrations, we obtain

$$\chi_\perp = \frac{b}{2H^2 T}\left[-1 + \frac{cH^2}{4b}g_\perp^2 + \left(1 + \frac{cH^2}{4b}g_\parallel^2\right)\left(\frac{1 + (cH^2/4b)g_\perp^2}{(cH^2/4b)(g_\perp^2 - g_\parallel^2)}\right)^{1/2}\right.$$

$$\times \tanh^{-1}\left(\frac{(cH^2/4b)(g_\perp^2 - g_{||}^2)}{1 + (cH^2/4b)g_\perp^2}\right)^{1/2}\right], \quad (11a)$$

$$\chi_{||} = \frac{b}{H^2 T}\left\{1 - \left[\frac{cH^2}{4b}\left(1 + \frac{cH^2}{4b}g_\perp^2\right)(g_\perp^2 - g_{||}^2)\right]^{-1/2}\right.$$

$$\left.\times \tanh^{-1}\left(\frac{(cH^2/4b)(g_\perp^2 - g_{||}^2)}{1 + (cH^2/4b)g_\perp^2}\right)^{1/2}\right\}. \quad (11b)$$

Expanding to lowest order in H^2, we obtain

$$\chi_\perp(H) = \frac{2}{3}\frac{c}{T}\left(\frac{-g_\perp^2 + \frac{1}{2}g_{||}^2}{4}\right.$$

$$\left. - \frac{1}{10}\frac{cH^2}{b}\frac{(g_\perp^2 - g_{||}^2)^2}{16} + \cdots\right), \quad (12a)$$

$$\chi_{||}(H) = \frac{2}{3}\frac{c}{T}\left(\frac{g_\perp^2 + \frac{1}{2}g_{||}^2}{4}\right.$$

$$\left. - \frac{4}{5}\frac{cH^2}{b}\frac{g_\perp^4 + \frac{1}{2}g_\perp^2 g_{||}^2 + \frac{3}{8}g_{||}^4}{16}\cdots\right). \quad (12b)$$

Equations (11b) and (12b) were given previously[4] for the case $g_{||} = 0$; for CMN the terms in $g_{||}$ may be safely neglected. The equations reduce to the usual Casimir–du Pré results for the case of an isotropic g factor.

III. EXPERIMENT

Susceptibility measurements were made on several specimens of CMN, each of which was inserted, in turn, into one of our standard thermometer coil formers, which was aligned with the coil axis in the horizontal plane. A description and illustration of the unit has been given elsewhere,[5] but some of the pertinent specifications are repeated. The coil system was made up of three coils; the two inner coils comprised the secondary and the outer coil the primary of a mutual inductance. Each section of the secondary was wound with No. 44 AWG ML insulated copper wire and was 1.78 cm long. The inner section had a mean diameter of 1.43 cm with a total of 2040 turns; the outer section had a mean diameter of 2.03 cm with a total of 1023 turns. The two sections of the secondary were connected in antiphase and were then balanced at room temperature relative to the primary to one part in 3000. The primary was wound of No. 40 AWG ML insulated copper wire, had a length of 3.66 cm and a mean diameter at the center of 2.14 cm. The primary had compensating windings at each end to produce a nearly uniform field over the length of the secondary (which was 0.5 cm longer than the specimen). The primary field (~0.05 G) was scanned with a test coil and was found to be 0.8% lower at the end of the secondary than at the center, rather than 0.1% as calculated. The static magnetic field was provided by a pair of Helmholtz coils which were mounted on a crude goniometer; the axis of the coils could

be adjusted such that it was perpendicular or parallel with the axis of the thermometer coils. This Helmholtz pair was calibrated to $\frac{1}{2}\%$ using a rotating-coil gauss meter.

To make the measurements, a specimen was inserted in the thermometer coils and the apparatus was then cooled to approximately 1.1 K by pumping on the helium bath. In the case of the single crystal, the c axis was aligned in the direction perpendicular to the plane of rotation of the Helmholtz pair so that there would be a susceptibility for both field directions. After the drift rate of the bath had diminished to about 0.1 mK/min, the susceptibility was measured in successively higher fields applied both parallel and transverse to the axis of the measuring coils. The susceptibility bridge used was a modification of one proposed by Maxwell[6] and was operated at 1700 Hz.

Since $\chi(H) \propto M(H) - M_0$ (where M is the mutual inductance of the bridge) is the experimental quantity sought, it was necessary to calibrate the system in zero field for each sample used in order to obtain the bridge constant M_0. The contribution from the Van Vleck temperature-independent susceptibility is lumped into the constant M_0.[7] It had been determined previously[4] that M_0 was independent of the applied field. The calibration was performed in the same manner as is customary for establishing a temperature scale, although in this case over a more limited temperature range. The He[4] bath was controlled at a predetermined pressure and the temperature was determined by measuring the vapor pressure of liquid ^{3}He. A least-squares fit of the bridge reading M to $1/T$ yielded the constants M_0 and A in the equation

$$M = A/T + M_0 .$$

For the frequency used, $\omega\tau \gg 1$ up to 1.6 K,[8] the maximum temperature of the calibration, so that the susceptibility was truly adiabatic.

Measurements were made on a sphere of compacted powder, a single crystal, and a cylinder of loose powder. The sphere was 1.270 cm in diameter and was machined from a cylindrical compact made of 80-vol% CMN and 20-vol% reagent-grade AgCl (< 10 ppm Fe). The single crystal was a slab $0.5 \times 1.1 \times 2.2$ cm; the loose powder was from the same material used for the compact but no AgCl was added. The packing fraction of the loose powder was not in excess of 0.65. The CMN was prepared from reagent-grade $Mg(NO_3)_2 \cdot 6H_2O$ and the best commercial $Ce(NO_3)_3 \cdot 6H_2O$, which contains about 1% other rare earths, principally La. The stoichiometry was established to 1% by analyzing for Mg and Ce (i.e., total rare earths).

The data for the various specimens are plotted as $(\chi_0 - \chi)/\chi$ vs $c'H^2/b$; here we have defined $c' \equiv \frac{1}{16}g_\perp^4 c$ where $c'/R = 3.82 \times 10^{-9}$ G^{-2} K^2. We have
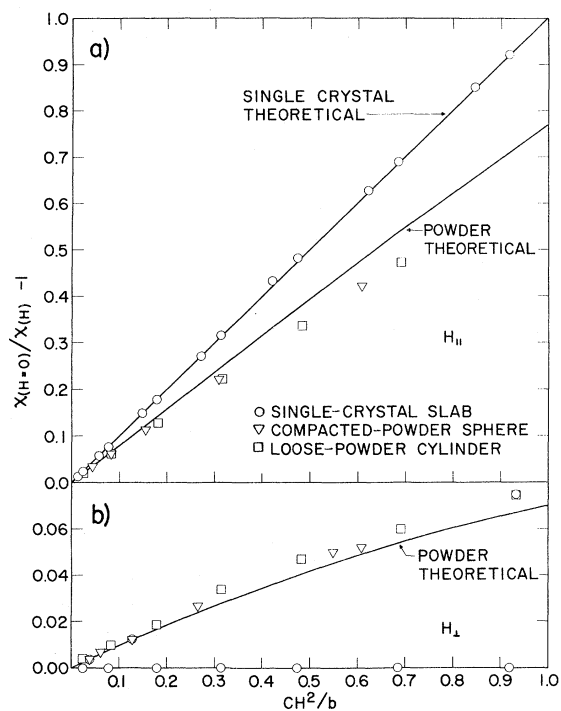
FIG. 1. Low-field plots of $\chi(H=0)/\chi(H) - 1$ vs $c'H^2/b$ for a single-crystal slab, compacted-powder sphere, and a loose-powder cylinder. The solid lines show the expected theoretical behavior. The upper and lower portions of the figure show, respectively, the behavior of the susceptibility measured parallel and perpendicular to the static field H.

taken $g_\perp = 1.84$ and $g_\parallel = 0$. Figure 1(a) illustrates the parallel and Fig. 1(b) the perpendicular components of the susceptibility at low fields. The corresponding high-field data are illustrated in Figs. 2(a) and (2b), respectively; here H is the applied field, and b is the leading term in the magnetic specific heat, $C_M = b/T^2 + \cdots$. We have used the single-crystal data to determine b and find b/R = $(6.16 \pm 0.1) \times 10^{-6}$ K^2. The value of b given by us in a previous publication[4] was 6.4×10^{-6}, which is 3% greater than the one given here. However, the previous value was determined on a powder over a more limited range of field; the new value 6.16 $\times 10^{-6}$ is, therefore, to be preferred. This value is also in excellent agreement with the recent value 6.10×10^{-6} quoted by Hudson and Pfeiffer,[9] which was obtained by thermal techniques.

One can see from Fig. 1 that the single crystal follows the Casimir–du Pré relation very well indeed. Further, there was no transverse field effect for the single crystal, as is to be expected from the theory. The data for the compacted and loose powders agree with each other but do not agree well with the theory for values of cH^2/b greater than 0.3. All comparisons between theory

and experiment for powders were made with Eqs. (11a) and (11b) rather than with the power-series expansions given in Eqs. (12a) and (12b). With the field applied in the parallel direction, the reduction in susceptibility is smaller than calculated, whereas with the field in the transverse direction the effect is greater than calculated. Careful tests were performed to rule out the possibility of misalignment between the measuring field and the applied field. A measure of the precision can be obtained from the fact that the correction for the earth's magnetic field deduced from the data, 0.78 G, was in excellent agreement with the measured value 0.8 G. To eliminate the possibility of spurious signals, the susceptibility was measured at 4.2 K in a field of 105 G applied in the parallel and transverse directions. Since $\omega\tau \ll 1$ at this temperature,[8] no field effect was expected and none was observed.

We wish to reiterate that the loose powder and the compacted powder with AgCl gave the same results. Thus, a rotation of the crystallites by
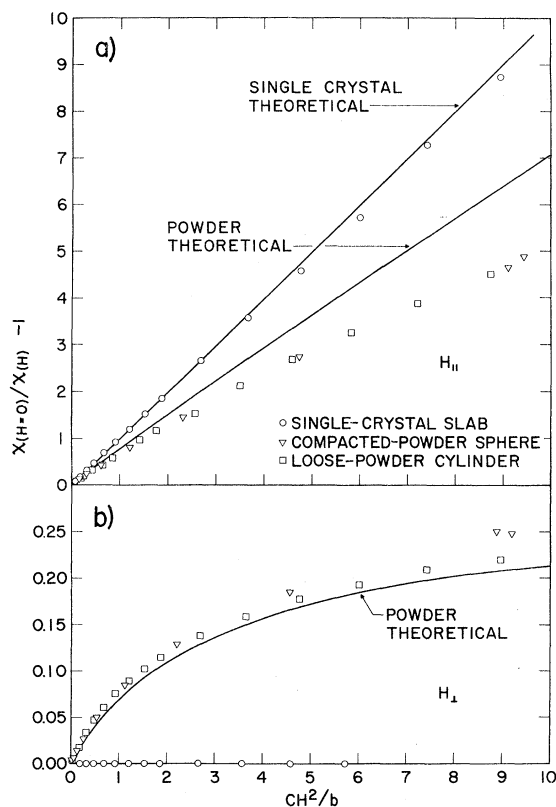

FIG. 2. High-field plots of $\chi(H=0)/\chi(H) - 1$ vs $c'H^2/b$ for a single-crystal slab, compacted-powder sphere, and a loose-powder cylinder. The solid lines show the expected theoretical behavior. The upper and lower portions of the figure show, respectively, the behavior of the susceptibility measured parallel and perpendicular to the static field H.

the static field would appear to be ruled out, since no such rotation is possible for a compacted powder with a binder. Further, the effect of the parallel and transverse fields is in the opposite direction for a simple correction. The fact that the single-crystal results agree with theory would argue against some peculiarity of the CMN itself (e. g., spin-lattice relaxation anomalies, [10] rare-earth impurities, etc.). Any discrepancies due to a difference between B and H should be negligible because of the small magnetization at the temperatures used here. The deviation of the experimental results on the powder from theory cannot be explained at this time.

*Work performed under the auspices of the U. S. Atomic Energy Commission.

[1]H. B. G. Casimir and F. K. du Pré, Physica 5, 507 (1938).

[2]J. C. Wheatley (private communication).

[3]Here we have used the English convention for Euler angles; cf. E. T. Whittaker, A Treatise on the Analytical Dynamics of Particles and Rigid Bodies (Dover, New York, 1964).

[4]B. M. Abraham, O. Brandt, Y. Eckstein, J. B. Ketterson, M. Kuchnir, and P. Roach, Phys. Rev. 187, 273 (1969).

[5]B. M. Abraham and Y. Eckstein, Phys. Rev. Letters 24, 663 (1970).

[6]E. Maxwell, Rev. Sci. Instr. 36, 533 (1965).

[7]The contribution from the Van Vleck temperature-independent susceptibility is additive under both adiabatic and isothermal conditions and may thus be lumped into the constant M_0. See J. C. Doran, U. Erich, and W. P. Wolf, Phys. Rev. Letters 28, 103 (1972).

[8]C. B. P. Finn, R. Orbach, and W. P. Wolf, Proc. Phys. Soc. (London) 77, 261 (1961).

[9]R. P. Hudson and E. R. Pfeiffer, in Proceedings of the European Physical Society Low Temperature Physics Conference, Freudenstadt, Germany (unpublished).

[10]R. P. Hudson and R. S. Kaeser, Physics 3, 95 (1967).

Defect Centers in Calcium Fluorophosphate

R. W. Warren

Westinghouse Research Laboratories, Pittsburgh, Pennsylvania 15235

(Received 20 April 1972)

Crystals of calcium fluorophosphate $Ca_{10}(PO_4)_6F_2$ have been grown from melts of various compositions. Optical and ESR measurements have been performed on samples before and after various treatments such as a uv irradiation and a thermal quench. Two kinds of defect centers have been detected: color centers produced by the irradiation, and more basic defects present in the samples before irradiation. The identity of two of these basic defects has been established and their role in the formation of the color centers has been deduced.

I. INTRODUCTION

Calcium fluorophosphate, often referred to as FAP, crystallizes in the hexagonal apatite structure and has a unit cell with the formula $Ca_{10}(PO_4)_6F_2$.[1] It has been investigated extensively partly because of its commercial importance as the phosphor in most fluorescent lamps and partly because of the richness of its defect structure and its color centers. Single crystals can be prepared by melt- or flux-growth techniques,[2-4] while powder samples similar to those used in lamps can be prepared by solid-state-reaction techniques. Optical measurements made on such crystals or on powders show strong absorption in the uv region of the spectra near 250 and 190 nm which is not a property of the perfect crystal since its strength is found to vary from sample to sample.[2,5] Owing to the magnitude of the absorption, it has been attributed not to trace impurities but to lattice defects or to some common impurity like oxygen or hydroxyl which might be incorporated in large amounts. Previous attempts to control its strength have been successful in powders but not in single crystals.[5]

Efforts have been made to identify the center (hereafter called the X center) responsible for the absorption at 250 nm (called the X band). John-son,[6] Swank,[7] and Piper, Kravitz, and Swank[8] have exposed crystals of fluorapatite to radiation from an x-ray source and have been able to partially convert the X center into various new defects. ESR measurements have been very successful[8] in identifying many of the paramagnetic defects made and can also be used to reveal the complex interac-